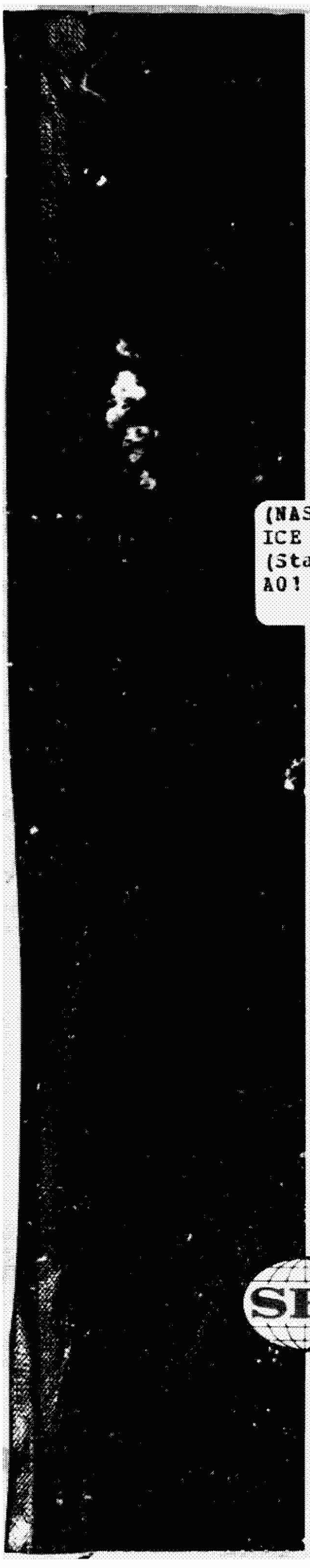

Final Report

MICROWAVE PROPERTIES OF ICE FROM THE GREAT LAKES

By: R. S. VICKERS

Prepared for:

NATIONAL AERONAUTICS & SPACE ADMINISTRATION
LEWIS RESEARCH CENTER
21000 BROOK PARK ROAD
CLEVELAND, OHIO 44135

Attention: R. GEDNEY

CONTRACT NAS 3-19092

STANFORD RESEARCH INSTITUTE
Menlo Park, California 94025 · U.S.A.

STANFORD RESEARCH INSTITUTE
Menlo Park, California 94025 · U.S.A.

Final Report *January 1975*

MICROWAVE PROPERTIES OF ICE FROM THE GREAT LAKES

By: R. S. VICKERS

Prepared for:

NATIONAL AERONAUTICS & SPACE ADMINISTRATION
LEWIS RESEARCH CENTER
21000 BROOK PARK ROAD
CLEVELAND, OHIO 44135
Attention: R. GEDNEY

CONTRACT NAS 3-19092

SRI Project 3571

Approved by:

DAVID A. JOHNSON, *Director*
Radio Physics Laboratory

RAY L. LEADABRAND, *Executive Director*
Electronics and Radio Sciences Division

Copy No. 200

ABSTRACT

The increasing use of radar systems as remote sensors of ice thickness has revealed a lack of basic data on the microwave properties of fresh-water ice. This report describes a program in which the complex dielectric constant was measured for a series of ice samples taken from the Great Lakes. The measurements were taken at temperatures of -5°, -10°, and -15°C. It is noted that the ice has considerable internal layered structure, and the effects of the layering are examined.

Values of 3.0 to 3.2 are reported for the real part of the dielectric constant, with an error bar of ±0.01.

CONTENTS

ILLUSTRATIONS

TABLES

I INTRODUCTION

The study of naturally occurring ice by airborne radar has been continuing since the inception of the early programs in remote sensing of earth resources a decade ago. The more recent work by Venier and Cross (1972) and Cooper et al. (1974) on lake ice has indicated a need for better fundamental data on microwave properties of this type of ice. Standard reference works such as Von Hippel (1954) quote values of the dielectric constant and loss tangent for ice at a number of isolated frequencies and temperatures, but for an understanding of the radar signatures of different ice types under naturally occurring conditions, more complete data are necessary. The measurements described in this report were made on samples of lake ice taken from Lake Erie by NASA personnel in the 1973-74 ice season.

II SAMPLE DESCRIPTION

The samples, which were in the form of cylindrical cores 3 inches in diameter and up to 36 inches in length, contained several broad categories of ice type:

(1) Clear ice

(2) Ice with inclusions 0.1 to 1 mm in diameter (milky in appearance)

(3) Ice with large irregular inclusions 0.1 to 0.6 cm in diameter.

Initially, attempts were made to find long enough sections of each sample to be representative of the whole core. This was not possible in most cases due to the highly fractured nature of the samples, and an alternative method of measuring the properties of the individual layers and computing the microwave properties of the whole sample was chosen. The NASA samples are described in detail in Table 1. One sample contained a small section of ice with verticle columns or pipes of entrapped air, but the size of this part of the sample was too small to allow measurement. All of the samples contained a substantial number of fractures and most of them consisted of a number of distinct layers of different appearance and air bubble content. Photographs of sections from four of the samples are given in Figures 1 through 4.

The frequency range employed for this study was 1 GHz to 18 GHz. Because of the inherent nature of commercial microwave equipment, it was necessary to perform the measurements in three separate ranges--namely, 1 to 8.2 GHz, 8.2 to 12.4 GHz, and 12.4 to 18 GHz. This in turn made it necessary to machine three samples out of each piece of ice to be measured. The low-frequency sample was mounted in a 1.625-inch coaxial transmission line, and the other samples were machined to fit into an appropriate waveguide section.

Table 1

DESCRIPTION OF ICE SAMPLES

NASA Sample No.	Length (cm)	Description
1	30	Clear. Fractured into lengths of 6 to 7 cm.
2	44	Inclusion 1 to 8 mm in strata 10 to 12 cm long. One clear section 10 cm long. Fractured.
3	47	Small inclusions, some small clear sections. Fractured into sections 8 to 12 cm long.
4	34	Mostly clear, occasional vertical striations. Fractured into sections 8 to 12 cm long.
5	34.5	Small inclusions, fractured.
6	45	Mostly clear, fractured into lengths of 7 to 8 cm.
7	47.5	Same as Sample No. 6.
8	75	Mostly clear. Bottom section crumbled and unusable. Fractured.
9	42	Clear, unevenly fractured into lengths of 3 to 5 cm.
10	78	Small inclusion (0.1 mm diameter), 7 cm snow cover. Fractured. 7 cm clear section. Occasional strata with inclusions up to 4 mm in diameter.

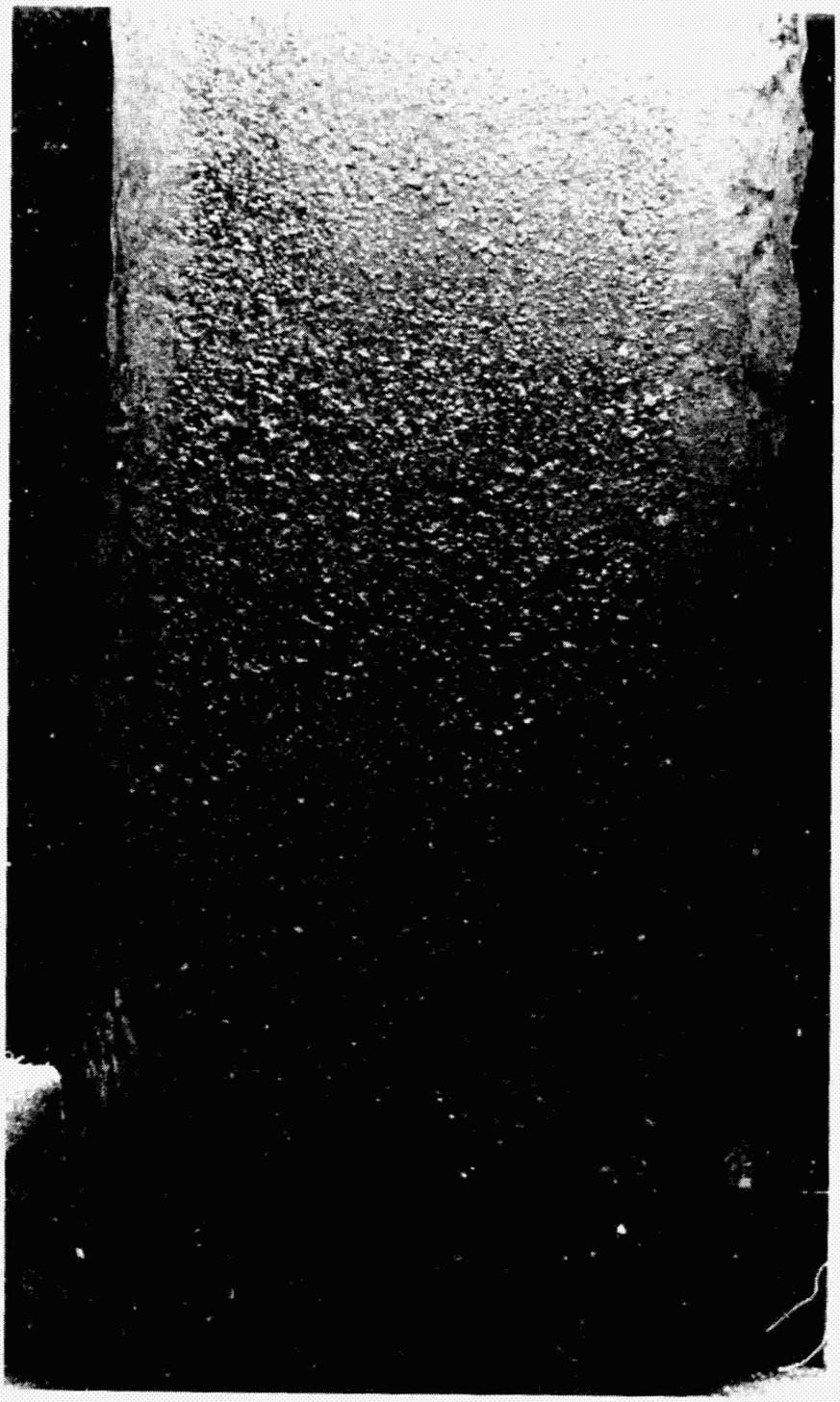

LA-3571-2

FIGURE 1 ICE SAMPLE 5 SHOWING SMALL INCLUSIONS

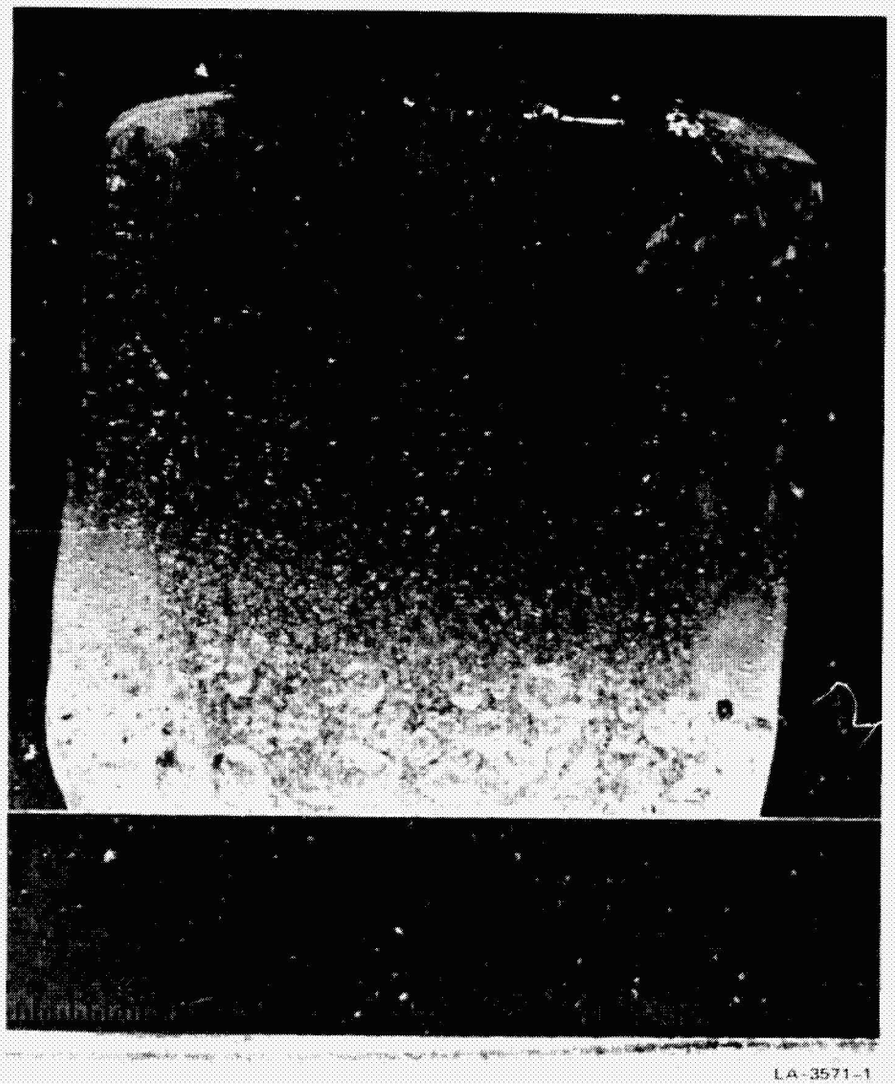

LA-3571-1

FIGURE 2 ICE SAMPLE 8 SHOWING CLEAR ICE WITH LAYERS OF LARGE INCLUSIONS

LA 3571-3

FIGURE 3 ICE SAMPLE 2 SHOWING HIGH DENSITY OF LARGE INCLUSIONS

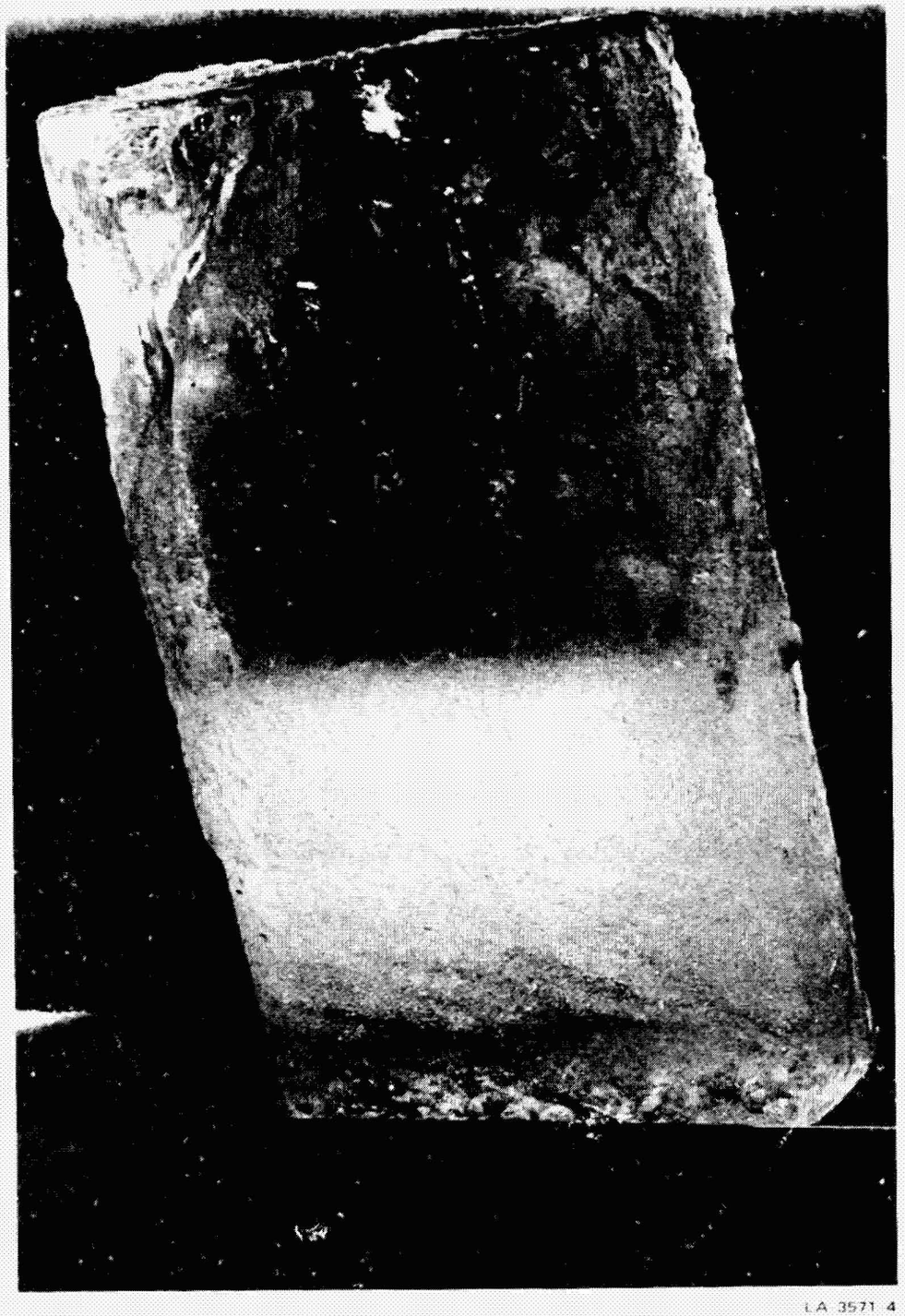

LA 3571 4

FIGURE 4 ICE SAMPLE 3 SHOWING LAYERS OF INCLUSIONS

III SAMPLE PREPARATION

Considerable difficulty was encountered in machining the ice samples to fit the various types of transmission line used for the measurements. It was found, for example, that the optimum temperature for machining was $-10^{o}C$. Warmer temperatures than this produced local melting as the ice was worked, and colder temperatures caused the ice to become excessively brittle. Figure 5 shows the coaxial samples being turned down on a lathe mounted in an environmental chamber set at $-10^{o}C$. The dimensional accuracy achievable was comparable to that obtained with conventional materials (i.e., ±0.001 inch). All samples were made 0.1 m in length. With this length of sample, using loss-tangent data from the literature, it was estimated that the sample losses would be just above the measurement limit of the network analyzer. Longer samples, although preferable, would have been difficult to select and fabricate, while shorter samples would not give a sufficiently high loss. The coaxial samples were first bored out to take the inner conductor of the transmission line, which was then frozen into place with the sample symmetrically positioned in the axial direction. The outer diameter of the ice was then machined and the outer conductor slid into place. Tapered transitions were then added to each end to enable the sample holder to be mated with the network analyzer.

For the frequency region 8.2 to 18 GHz samples were machined to fit 0.1-m lengths of X- and P-band waveguide. Initial cutting was done on a bandsaw. Further preparation was done with fine sandpaper and a series of jigs to ensure a tight fit into the waveguide. It can be seen that for one set of measurements over the full frequency range, at least 0.3 m of the ice sample had to be of the same type, and had to have no severe fracturing present. Following the assembly of the samples in the holders, the samples were taken to the analyzer facility and allowed to come to equilibrium at $-5^{o}C$ prior to the start of the measurements.

FIGURE 5 COAXIAL ICE SAMPLE BEING MACHINED IN AN ENVIRONMENTAL CHAMBER

IV MEASUREMENT PROCEDURE

The measurement procedure used initially for the Great Lakes ice samples is described in detail in the Appendix. In summary, the method consists of injecting a continuous microwave signal into the sample, and measuring the phase and amplitude of both the reflected and transmitted waves as the input frequency is swept over the range of interest. The network analyzer (a computer-controlled H-P 8541A) then calculates the reflection coefficient for an infinite sample, and the loss tangent and complex dielectric constant for the material. The procedure could be extended over any frequency range between 1 and 18 GHz in steps of one octave.

The sample temperature was controlled by two thermoelectric coolers, and was continuously displayed during the measurement. Three temperatures were chosen; these were -5°, -10°, and -15°C. In retrospect, an upper limit in temperature closer to the melting point would have been more appropriate in view of typical conditions in the spring on the Great Lakes.

Some trouble was continually encountered in the precision connectors from the sample holder to the analyzer, in that any cooling of these devices produced errors in the phase measurements on the sample. This will be discussed further under the section on errors.

The analyzer was limited to approximately 40 frequency points per measurement which, in effect, meant that frequency points tended to be spaced by 100 to 150 MHz. Fortunately, none of the electrical properties of ice appear to be a strong function of frequency in the range covered by this investigation, and the spacing was therefore accepted as adequate. To start a data run the equipment was calibrated extensively in order to remove the propagation effects of the sample holder and its connectors. Further checking of the equipment was also achieved by measuring the properties of a Teflon sample and comparing the results with known values.

After the completion of these formal test procedures the samp e holder with the ice in place was connected and allowed to come to equilibrium at $-5^{\circ}C$. The properties of the ice sample were then measured and the experiment repeated for temperatures of $-10^{\circ}C$ and $-15^{\circ}C$. Because of the time necessary to change temperature and come to equilibrium, the measurement of one sample would take from 4 to 5 hours, and one day's operation would usually result in only two samples being completed. Figure 6 shows the sample holder for the 1 to 8.2 GHz measurements, and the network analyzer is shown in operation in Figure 7. In this figure, the thermoelectric coolers can be seen on top of the cold chest.

LA-3671-6

FIGURE 6 SAMPLE HOLDER FOR THE 1-TO-8-GHz MEASUREMENT

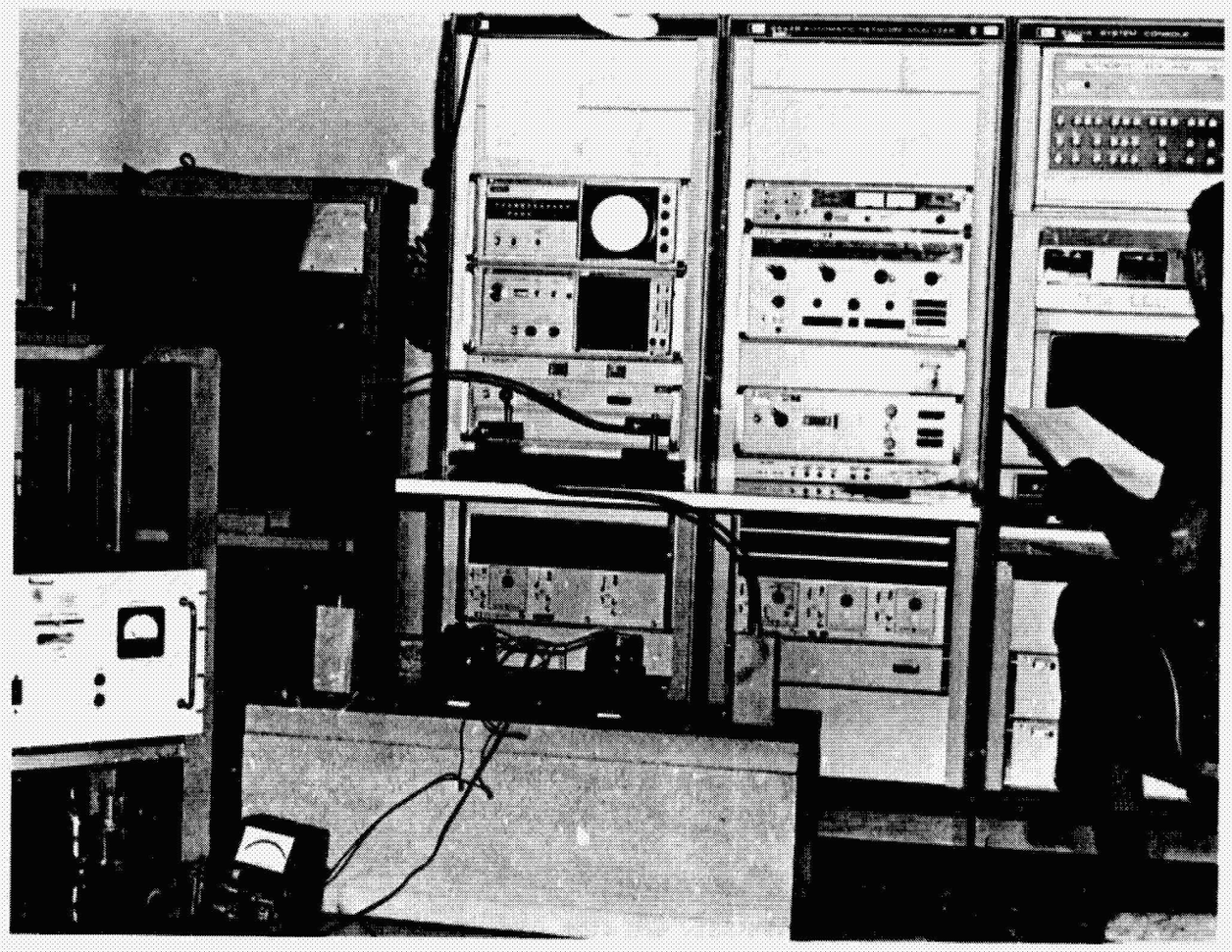

LA-3571-7

FIGURE 7 SRI NETWORK ANALYZER PERFORMING MEASUREMENTS ON ICE SAMPLES

V DATA REDUCTION

The majority of the data were reduced using the method described in the Appendix. An example of the output from this process appears in Figure 8.

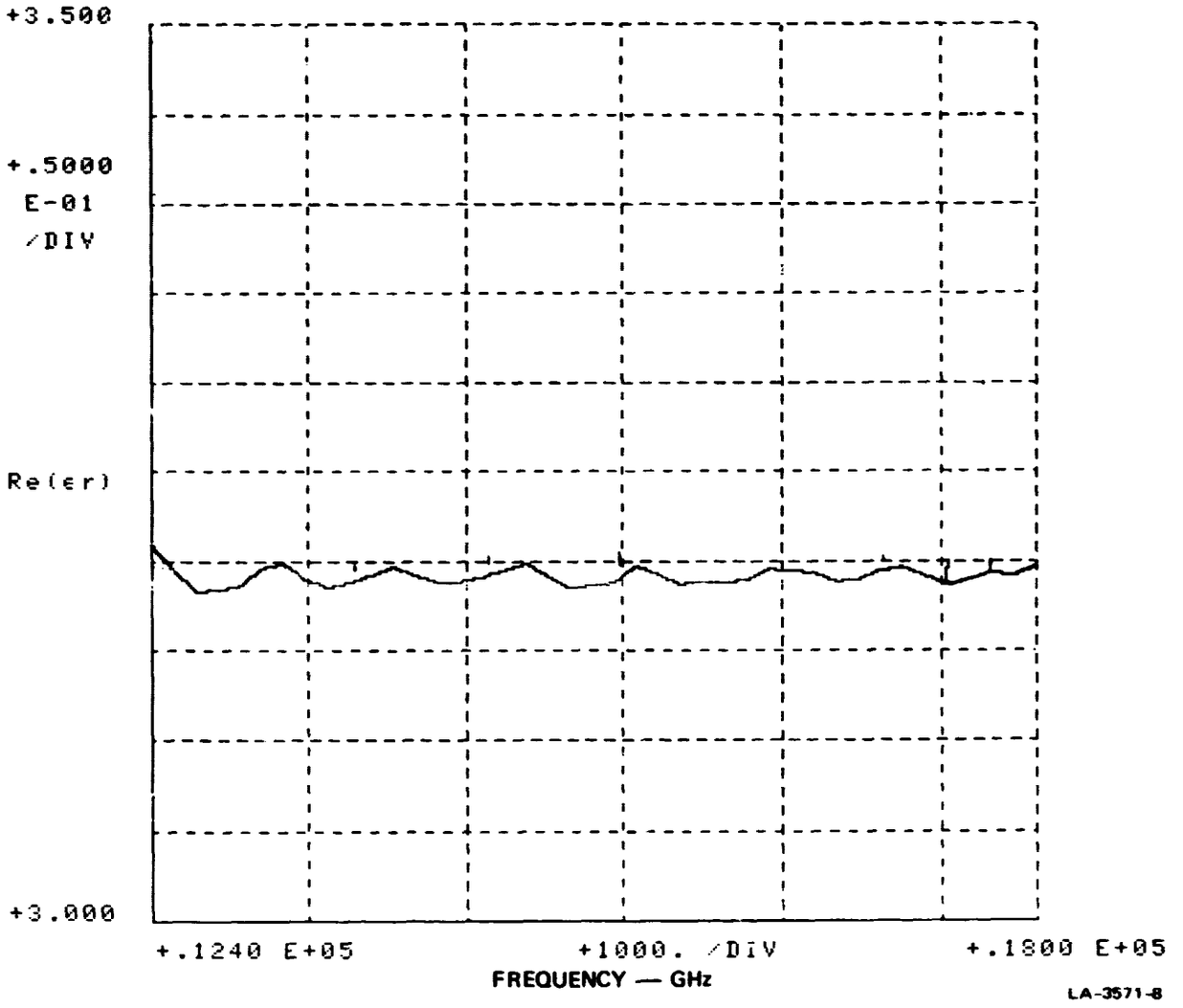

FIGURE 8 EXAMPLE OF OUTPUT FROM SCATTERING-PARAMETER PROGRAM

The options for output format include plots of loss tangent, losses in dB/m, absorption coefficient, permeability, and real and imaginary parts of the dielectric constant. Of these, the absorption losses in dB/m and the real part of the dielectric constant were chosen as being of the greatest value. The permeability of ice was of course unity for all frequencies. In the case of data from 1 to 8.2 GHz, an alternative scheme of calculating the dielectric properties from the transmitted wave alone was found necessary because of the low losses in ice, which allowed multiple reflections and standing waves to be set up within the sample. On occasion this allowed the ice to act as a quarter-wave plate giving reflection coefficients of zero, which in turn caused the conventional program to divide by zero and rendered large segments of the data unusable.

In the alternative program the real part of the dielectric constant is given by differentiating the phase of the transmitted signal with respect to frequency. This gives the group delay of the wave, and hence the real part of ϵ_r, as indicated by Eq. (11) in the Appendix. An example of a typical phase plot is given in Figure 9 in which it can be seen that the slope varies little over the entire frequency range, giving an almost constant value for ϵ_r. The cyclic variations are caused by the multiple reflections within the sample, and have to be removed by smoothing before the dielectric constant is calculated.

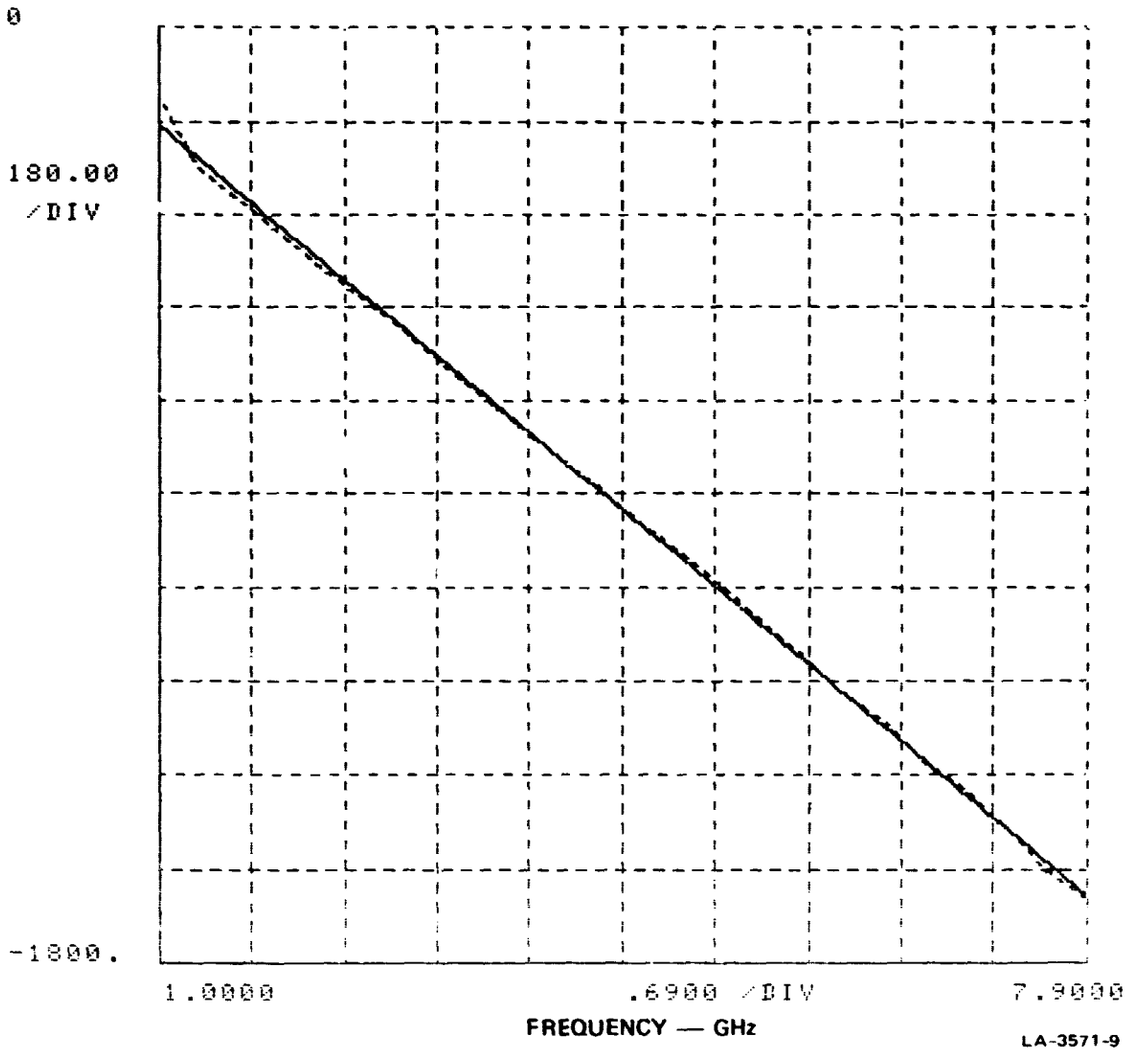

FIGURE 9 EXAMPLE OF PHASE PLOT VERSUS FREQUENCY FOR AN ICE SAMPLE

VI RESULTS

The ice samples from the Great Lakes contained several different types of ice, as explained earlier in this report. All the samples had a layered structure, and most included strata of several different ice types. For the purpose of this report the ice was classified as clear, milky with small inclusions, or clear with large inclusions. Measurements under a microscope indicated that the "milky" classification typically contained over 500 inclusions/cm^3 with diameters of 10^{-2} cm, and in most cases also included over 9/cm^3 with diametersof 5×10^{-2} cm. Using a mixing rule on these numbers, and taking the ϵ_r as 3.2 for pure ice, the bulk dielectric constant for the samples would be 3.19 for the small inclusions and 3.12 for the samples with both sizes of inclusions. The samples with large inclusions typically contained air bubbles with diameters of 0.6 cm at a density of 0.62/cm^3. Using the mixing rule as before, the predicted value for ϵ_r would be 3.05.

A number of samples of each of these types were measured, and the results are given in Figures 10, 11, and 12. The discontinuities in the plots occur at points where the increasing frequency necessitated a new sample holder and sample, and correspond to 1 to 8.2 GHz (coaxial transmission line), 8.2 to 12.4 GHz (X-band waveguide), and 12.4 to 18 GHz (P-band waveguide). The error bars on these measurements are larger than was hoped, primarily due to the effects of the temperature change on the precision cables and connectors and the resonant effects in the low-loss ice samples. It is easily seen that in the case of solid ice the real part of the dielectric constant is not a strong function of frequency, and neither is the dielectric loss, expressed here as attenuation in dB/m. An important observation from the standpoint of remote sensing is that the ice is virtually loss over the entire range from 1 to 18 GHz, and that one should not therefore limit the bandwidth and resolution of airborne

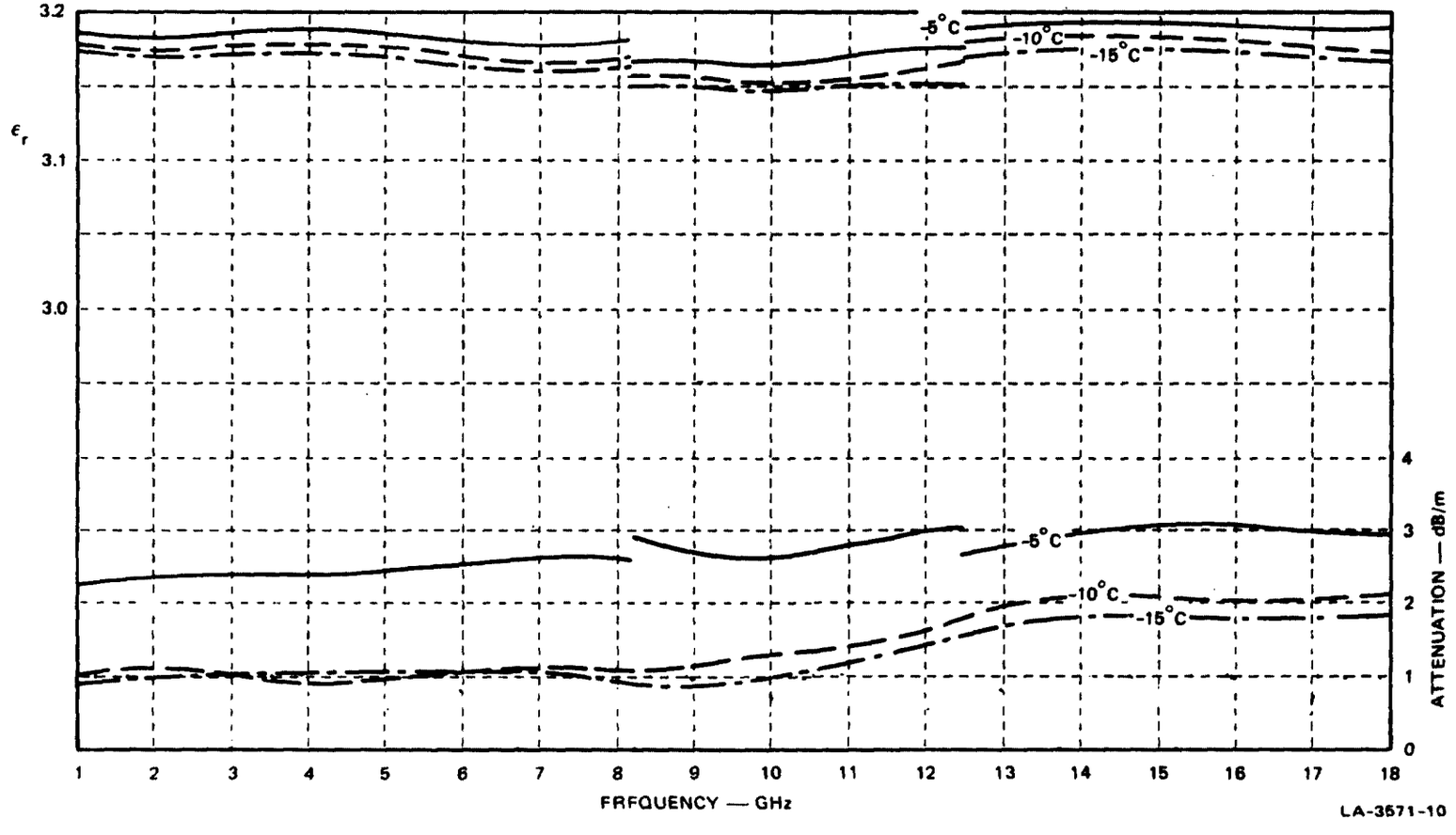

FIGURE 10 MICROWAVE PROPERTIES OF LAKE ICE WITH NO INCLUSIONS

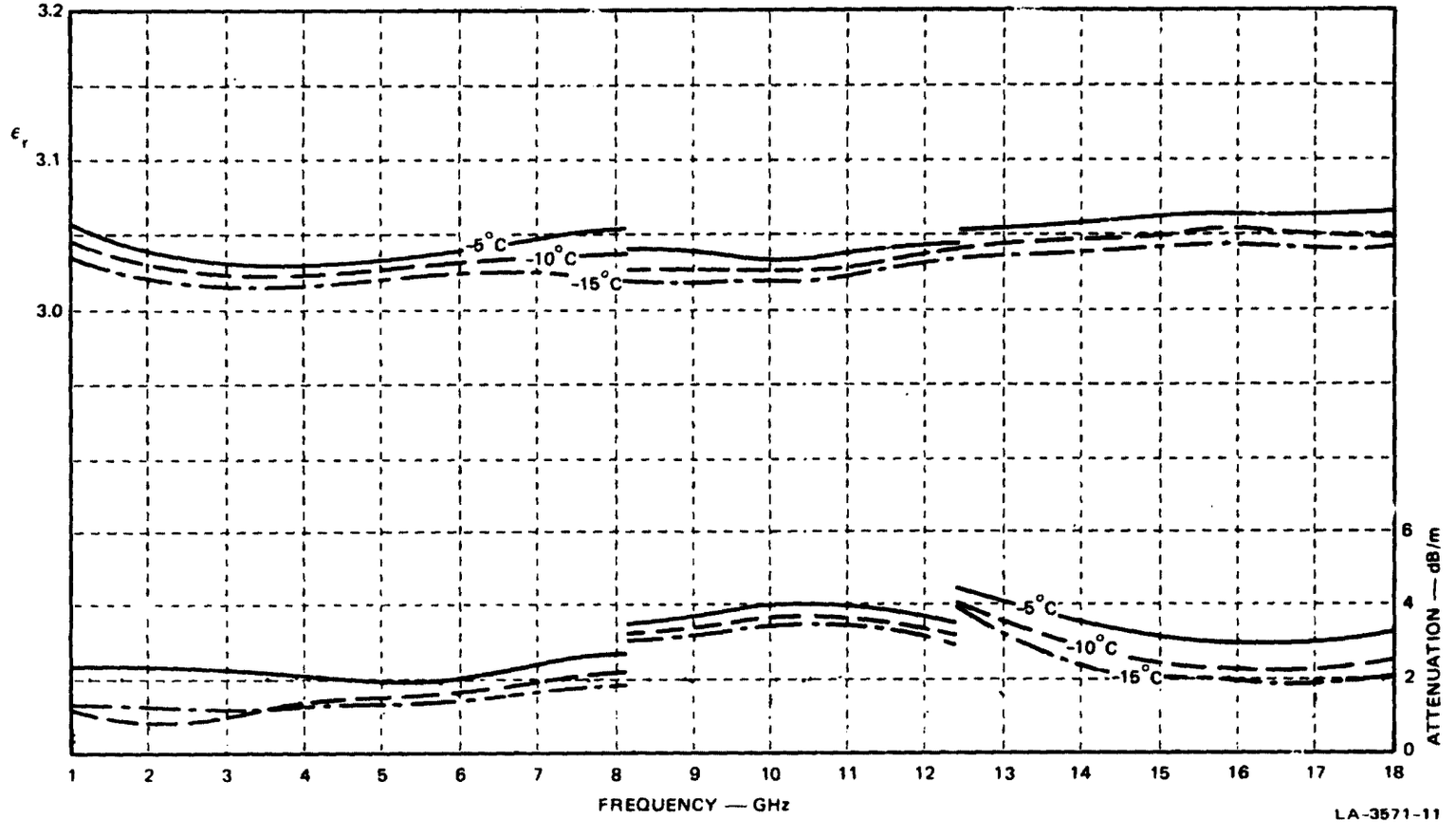

FIGURE 11 MICROWAVE PROPERTIES OF LAKE ICE WITH SMALL INCLUSIONS

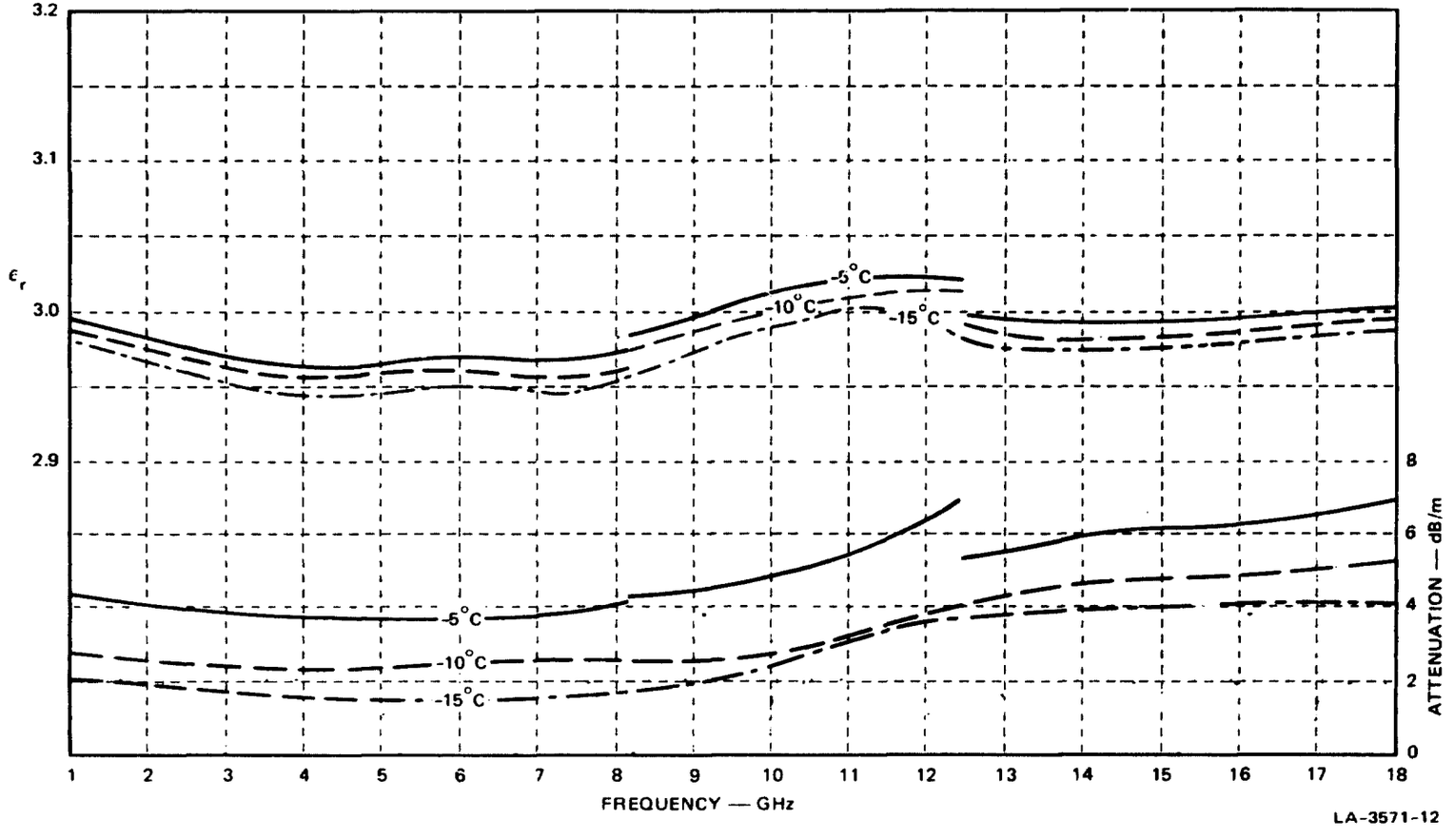

FIGURE 12 MICROWAVE PROPERTIES OF LAKE ICE WITH LARGE INCLUSIONS

profiling techniques because of loss considerations in the ice. The losses encountered in the samples that had a significant volume of inclusions are clearly due to a scattering process rather than to dielectric absorption.

The magnitude of the losses was for the most part below the noise level of the network analyzer, and in all cases was less than 8 dB/m. This was a somewhat surprising result and would have no doubt been different if we had performed the measurements closer to the melting point of the ice. For comparison, Von Hippel (1954) quotes a value of 1.1 dB/m for pure ice at -12^{o}C. Tables 2 and 3 show the dielectric properties of the ten NASA samples constructed from measurements of their stratigraphy and the microwave measurements on individual layers taken from the samples. One measured sample is not included in these results. It was a section from NASA Sample 2, which gave a measured value of ϵ_r of 3.65. The measurement was not repeatable due to deterioration of the sample, and the result did not fit the trend for other ice measurements and was therefore ignored.

It was noted that the effect of temperature of the real part of the dielectric constant was negligible, and was within the error bars for the experiment. This supports the work of Cumming (1952), who maintained that temperature was not an important parameter at 10 GHz for ice and snow measurements. A trend was noted, however, where ϵ_r would increase by $0.002/^{o}$C. It is hard to determine whether this was a real trend or whether it was due to temperature variations within the connectors and cables. For the temperature range under consideration it was in any case a very minor effect.

In the case of dielectric loss, there was a consistent increase in loss as the temperature increased. None of the losses measured were greater than 8 dB/m at -5^{o}C. Greater losses would have no doubt been detected at temperatures closer to the melting point.

Table 2

VALUES OF ϵ_r FOR NASA SAMPLES AT $-5^{\circ}C$*

Frequency (GHz)	NASA Sample No.						
	1 and 9	2	3	4,6,and 7	5	8	10
1	3.18	3.03	3.06	3.17	3.04	3.13	3.04
2	3.18	3.03	3.07	3.17	3.04	3.18	3.04
3	3.18	3.02	3.07	3.17	3.03	3.14	3.03
4	3.19	3.02	3.06	3.17	3.03	3.14	3.03
5	3.18	3.02	3.06	3.17	3.04	3.13	3.04
6	3.17	3.02	3.06	3.16	3.04	3.12	3.04
7	3.17	3.02	3.07	3.16	3.05	3.12	3.05
8	3.17	3.02	3.07	3.16	3.05	3.13	3.05
9	3.15	3.03	3.06	3.14	3.04	3.11	3.04
10	3.12	3.03	3.05	3.11	3.03	3.09	3.03
11	3.14	3.04	3.06	3.13	3.04	3.11	3.04
12	3.15	3.05	3.08	3.14	3.05	3.12	3.05
13	3.16	3.05	3.07	3.16	3.06	3.12	3.05
14	3.18	3.04	3.08	3.17	3.06	3.14	3.06
15	3.18	3.04	3.08	3.17	3.07	3.14	3.06
16	3.18	3.04	3.08	3.17	3.07	3.14	3.06
17	3.18	3.05	3.09	3.17	3.07	3.14	3.06
18	3.18	3.05	3.09	3.17	3.07	3.14	3.07

*Values have been rounded to three significant figures and are all subject to a total error of ±0.01. For values at $-10^{\circ}C$, subtract 0.01 from all readings. For values at $-15^{\circ}C$, subtract 0.02.

Table 3

ATTENUATION OF NASA SAMPLES AT -5°C*

(dB/m)

Frequency (GHz)	NASA Sample No.						
	1 and 9	2	3	4,6, and 7	5	8	10
1	2.4	3.6	2.5	2.4	2.1	2.5	2.5
2	2.4	3.6	2.5	2.4	2.2	2.5	2.6
3	2.4	3.6	2.5	2.4	2.1	2.5	2.5
4	2.4	3.5	2.4	2.4	2.0	2.5	2.4
5	2.4	3.5	2.4	2.4	2.0	2.5	2.4
6	2.5	3.5	2.4	2.5	2.0	2.5	2.4
7	2.5	3.6	2.7	2.5	2.4	2.7	2.8
8	2.6	3.7	2.9	2.6	2.7	2.8	3.0
9	2.6	3.9	3.4	2.7	3.2	3.0	3.5
10	2.6	4.3	3.8	2.8	4.0	3.1	4.0
11	2.8	4.8	3.8	2.9	3.8	3.3	4.0
12	3.0	5.3	3.9	3.1	3.7	3.4	4.1
13	3.0	5.3	3.8	3.0	3.5	3.4	4.0
14	2.9	5.2	3.7	3.0	3.4	3.3	3.9
15	2.9	5.3	3.6	3.0	3.2	3.3	3.7
16	3.0	5.4	3.5	3.0	3.0	3.3	3.6
17	3.0	5.6	3.5	3.0	3.0	3.3	3.7
18	2.9	5.8	3.6	2.9	3.1	3.3	3.8

*These values are subject to an error of ±1.5 dB/m. Values at -10°C were consistently 1 dB/m lower than the value shown. Attenuation at -15°C was close to the noise level of the Network Analyzer and was approximately 1.5 dB/m less than the values shown here.

VII MEASUREMENT ERRORS

Two important sources of possible error were present in this measurement program--sample preparation, and computational errors. In the waveguide measurements (from 8.2 to 18 GHz), the samples were accurately fitted and any errors in sample fabrication were due to the final facing operation which tended to open up any inclusions near the surface and leave nonplanar interfaces. In the case of the coaxial measurements (1 to 8.2 GHz) the problem was that the inner conductor could produce chipping around the end faces of the sample, and these were difficult to "repair" accurately.

The dominant source of error in the whole program was the fundamental problem of measuring phase accurately in the presence of multiple internal reflections within the ice sample. Over a bandwidth of 1 GHz, for example, an error in the measurement of the phase of the transmitted wave of 1^{o} produces an error in ϵ_r of 0.003. Under normal conditions, using medium-to-high-loss samples, the network analyzer is capable of phase accuracies of 1^{o}. With ice, however, the low losses allow the generation of standing waves within the sample that modify the phase of the emerging wave and cause phase measurement errors of $\pm 2^{o}$. This produces an uncertainty of ± 0.006 in ϵ_r. The measurement of losses within the ice sample was affected in the same way, but was limited by the noise level of the network analyzer, which effectively produced a lower limit of 0.1 dB on all loss measurements. Since all the ice samples were 0.1 m in length, the lower limit was therefore 1 dB/m. An additional uncertainty was introduced by the effects of cooling on the cables and connectors leading to the sample area. Experiments on an emply sample holder were conducted to establish the magnitude of this effect, and the results lead to a total figure of ± 1.5 dB/m for the errors in the attenuation data.

VIII CONCLUSIONS

The samples used in this study did not produce any dramatic unexpected results. The real part of the dielectric constant varied from approximately 3.0 to 3.2 and was dependent on the volume of air inclusions present in the sample. Temperature did not affect this parameter noticeably. Dielectric loss varied from 2 dB/m to 8 dB/m, and was also primarily a function of inclusions rather than temperature. The forward loss was therefore due to a scattering mechanism and not to the conductivity of the sample.

It is reasonable, therefore, to assume that the backscatter in the samples would be proportional to the measured attenuation at any given frequency for the samples.

In no case did we find any properties that would explain anomalous backscatter as observed by NASA's sidelooking radar, or a sufficiently high value for permittivity that could substantiate the value of 4.0 used in early flight tests to obtain a closest fit between the ice thickness and the short-pulse-radar results.

It is felt that with further work on new samples, the error bars on the microwave data reported here could be reduced substantially by use of improved measurement techniques.

Appendix

Automatic Measurement of Complex Dielectric Constant and Permeability at Microwave Frequencies

WILLIAM B. WEIR, MEMBER, IEEE

***Abstract*—With the advent of the computer and automatic test equipment, new techniques for measuring complex dielectric constant (ϵ) and permeability (μ) can be considered. Such a technique is described where a system is employed that automatically measures the complex reflection and transmission coefficients that result when a sample of material is inserted in waveguide or a TEM transmission line. Measurement results of ϵ and μ for two common materials are presented.**

Introduction

THE MEASUREMENT of complex dielectric constant and complex permeability is required not only for scientific but also for industrial applications. For example, areas in which knowledge of the properties of materials at microwave frequencies (as described by ϵ and μ) are applications of microwave heating, biological effects of microwaves, and nondestructive testing.[1]

Numerous measurement methods suitable for different ranges of the numerical values of ϵ and μ have been given in the books edited by Von Hippel [2], [3] and in publications of the American Society for Testing and Materials. It is possible, however, to rapidly make measurements over the frequency range from 100 MHz to 18 GHz with a computer-controlled network analyzer such as the Hewlett-Packard Model 8540 series, and by means of appropriate data processing, to determine the complex values of ϵ and μ for materials.

Using the method described in this paper, the complex values of ϵ and μ are determined from measurements made directly in the frequency domain. A somewhat analogous method has been developed [7] where measurements are made in the time domain of the transient response to subnanosecond pulses from a dielectric material. With the time-domain measurement approach, a Fourier transformation is required to determine ϵ and μ from the measured transient response. Furthermore, with this approach, the frequencies at which ϵ and μ values are obtained are band-limited, depending on the time response of the pulse and its repetition frequency. Using the system described in this paper, discrete frequencies in less than 20-kHz steps may be selected anywhere within the entire 100-MHz to 18-GHz band.

Automatic Measurement System

A computer-controlled network analyzer is used to measure the parameters of a network consisting of a section of transmission line containing the sample of material. The transmission line section may either be waveguide or a TEM transmission line. The network is shown schematically in Fig. 1. If coaxial-to-waveguide adapters are required, additional lengths of waveguide are inserted between them and the sample holder. This is to insure that the higher order evanescent modes due to the coaxial-to-waveguide adapters are significantly attenuated prior to reaching the sample under test.

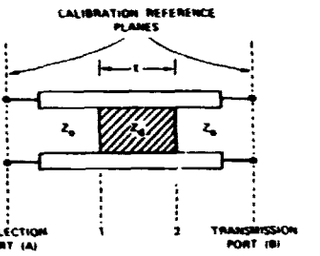

Fig. 1. Transmission line section containing dielectric material.

Under computer control, network analyzer system calibration and measurement are obtained at the reference planes indicated in Fig. 1. This is done over a number of predetermined frequencies at which the complex values of ϵ and μ for the material are to be determined. The normalized scattering parameters (S_{ij}) of the transmission line section containing the material are measured at the calibration reference planes at ports A and B and corrected for system errors included in the calibration data. The measured scattering parameters are normalized to the characteristic impedance (Z_0) of the transmission line section. The reflection coefficient (S_{11}) at the air-to-dielectric interface, and the transmission coefficient (S_{21}) through the material, are found at reference planes 1 and 2. These coefficients are found directly from the measured scattering parameters after the appropriate phase corrections have been applied to account for the shift in the reference planes from ports A and B to the material interfaces (i.e., planes 1 and 2, Fig. 1).

From the complex reflection and transmission coefficients, the computer associated with the network analyzer determines the real and imaginary parts of the dielectric constant and permeability, the loss tangent, and the attenuation per unit length of material. In addition, data taken at several frequencies are used to find the average group delay through the sample. Average group delay, in turn, is used to automatically resolve phase ambiguities that result when the sample length of material is greater than a wavelength in the dielectric. The complex ϵ and μ, loss tangent, and attenuation data are automatically listed by a teleprinter, or rapidly plotted on an X–Y recorder, or both.

Data Processing Techniques

The equations used to compute complex ϵ and μ from the measured reflection (S_{11}) and transmission (S_{21}) coefficients are presented below together with the equations that relate ϵ

Manuscript received April 17, 1973; revised July 9, 1973.

The author is with Stanford Research Institute, Menlo Park, Calif. 94025.

[1] For an example of a system that can be used for nondestructive testing see [11].

and μ to attenuation and loss tangent. As will be seen, an infinite number of roots exist in the solution for the equations ϵ and μ, but the correct root is related to the length of the sample in terms of wavelength within the material. The means of determining the correct solution is shown.

Referring to Fig. 1, the propagation factor for a wave propagating through the material is defined as [4]

$$P = e^{-\gamma l} = e^{-(\alpha+j\beta)l} \tag{1}$$

where

γ propagation constant,
α attenuation constant,
β phase constant.

A time factor of $e^{j\omega t}$ is not explicitly shown in (1). The phase constant is equal to

$$\beta = \frac{2\pi}{\lambda_g} \tag{2}$$

where λ_g is the transmission line guide wavelength. Consistent with the definition of the propagation factor [(1)], ϵ and μ are defined in terms of their real and imaginary parts as follows:

$$\epsilon = \epsilon_r\epsilon_0 = (\epsilon_r' - j\epsilon_r'')\epsilon_0 \tag{3}$$

$$\mu = \mu_r\mu_0 = (\mu_r' - j\mu_r'')\mu_0. \tag{4}$$

The reflection coefficient (Γ) at the interface between the air-filled transmission line and dielectric-filled line when the material sample is infinite in length may be found from the measured reflection (S_{11}) and transmission (S_{21}) coefficients for a sample of finite length (l):[2]

$$\Gamma = \chi \pm \sqrt{\chi^2 - 1} \tag{5}$$

where

$$\chi = \frac{S_{11}^2 - S_{21}^2 + 1}{2S_{11}}. \tag{6}$$

The propagation factor P can, in turn, be found from S_{11}, S_{21}, and Γ:

$$P = \frac{S_{11} + S_{21} - \Gamma}{1 - (S_{11} + S_{21})\Gamma}. \tag{7}$$

The complex dielectric constant and permeability can be determined from P and Γ:

$$\frac{1}{\Lambda^2} = \left(\frac{\epsilon_r\mu_r}{\lambda_0^2} - \frac{1}{\lambda_c^2}\right) = -\left[\frac{1}{2\pi l}\ln\left(\frac{1}{P}\right)\right]^2 \tag{8}$$

$$\mu_r = \frac{1+\Gamma}{\Lambda(1-\Gamma)\sqrt{\dfrac{1}{\lambda_0^2} - \dfrac{1}{\lambda_c^2}}} \tag{9}$$

where

λ_0 free space wavelength,
λ_c cutoff wavelength of the transmission line section ($\lambda_c = \infty$ for a TEM line),

and

$$\mathrm{Re}\left(\frac{1}{\Lambda}\right) = \frac{1}{\lambda_g}.$$

Equation (8) has an infinite number of roots since the imaginary part of the logarithm of a complex quantity [P in (8)] is equal to the angle of the complex value plus $2\pi n$, where n is equal to the integer of (l/λ_g). Equation (8) is ambiguous because the phase of the propagation factor P does not change when the length of the material is increased by a multiple of wavelength. However, the delay through the material is strictly a function of the total length of the material and can be used to resolve the ambiguity.

The phase ambiguity is resolved by finding a solution for ϵ and μ from which a value of group delay is computed that corresponds to the value determined from measured data at two or more frequencies. For this method to work, the discrete frequency steps at which measurements are obtained must be small enough so that the phase of the propagation factor (P) changes less than 360° from one measurement frequency to the next. With the use of an automatic measurement system as described in this paper, discrete frequency steps, small enough to meet this requirement, can easily be selected. The group delay at each frequency may be computed for each solution of ϵ and μ assuming that the changes in ϵ and μ are negligible over very small increments of frequency:

$$\tau_{gn} = l\frac{d}{df}\left[\left(\frac{\epsilon_r\mu_r}{\lambda_0^2} - \frac{1}{\lambda_c^2}\right)_n^{1/2}\right] \tag{10}$$

where f is the frequency in hertz and τ_{gn} is the group delay in seconds for the nth solution of (8) and (9). The measured group delay is determined from the slope of the phase of the propagation factor versus frequency:

$$\tau_g = \frac{1}{2\pi}\frac{d(-\phi)}{df} \tag{11}$$

where ϕ is the phase in radians of P. Accuracy in the determination of τ_g may be increased by applying numerical differentiation techniques [5] where the slope is computed using data for three or more frequencies. The correct root, $n = k$, is found when

$$\tau_{gk} - \tau_g \simeq 0.$$

Once the correct values of ϵ and μ have been found at each of the measurement frequencies, the loss tangent and attenuation per unit length may be determined. In general, for both an electrically and magnetically lossy material, a loss tangent is defined by[3]

$$\tan\delta = \frac{\delta_r''}{\delta_r'} \tag{12}$$

where

$$\delta_r' = \mu_r'\epsilon_r' - \mu_r''\epsilon_r''$$

[2] In terms of the air-filled line characteristic impedance Z_0 and the dielectric-filled line characteristic impedance Z_d, $\Gamma = (Z_d - Z_0)/(Z_d + Z_0)$. Note that $S_{11} = \Gamma$ when l is infinite.

[3] Note that for the case when $\mu_r'' = 0$, $\tan\delta = \epsilon_r''/\epsilon_r'$.

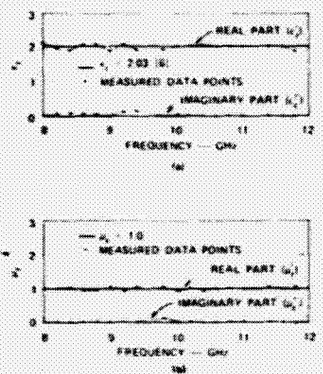

Fig. 2. Measured dielectric constant and permeability of Teflon in the X-band region. (a) Relative dielectric constant (ϵ_r). (b) Relative permeability (μ_r).

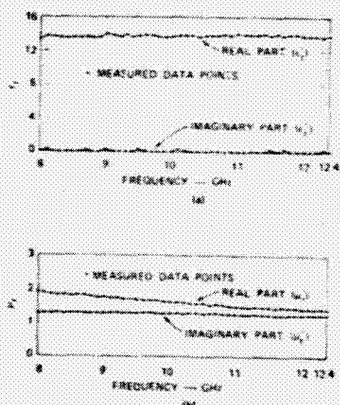

Fig. 3. Measured dielectric constant and permeability of Eccosorb SF-5.5 in the X-band region. (a) Relative dielectric constant (ϵ_r). (b) Relative permeability (μ_r).

and

$$\delta_r'' = \mu_r'\epsilon_r'' + \mu_r''\epsilon_r'.$$

The attenuation in nepers per length is found from the equation

$$\alpha = \frac{\pi\sqrt{2\delta_r'}}{\lambda_0}\left[\sqrt{1+\tan^2\delta}-1\right]^{1/2}. \qquad (13)$$

Measured Results

The results of measuring the complex ϵ and μ of Teflon and Emerson and Cuming Eccosorb SF-5.5 are shown in Figs. 2 through 4. Measurements of both materials were obtained with a sample inserted in X-band (RG-52) waveguide and at an ambient temperature of 22°C. The Teflon sample length was 1 in; the Eccosorb sample length was 0.090 in.

Teflon has a relatively low ϵ_r' (2.03 [6]) in the microwave region and has a very low loss at X band ($\tan\delta < 0.0004$ [2]). It is a nonmagnetic material and hence its relative permeability (μ_r) is 1. The measured data shown in Fig. 2 correspond closely to these known properties of Teflon.

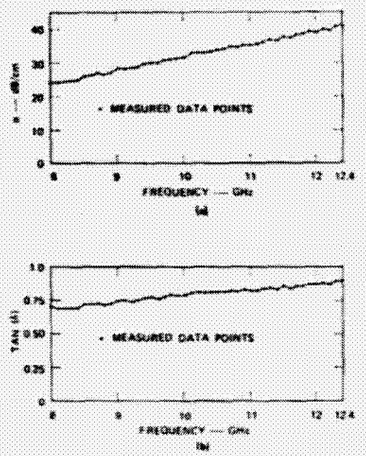

Fig. 4. Measured attenuation and loss tangent of Eccosorb SF-5.5 in the X-band region. (a) Attenuation (α). (b) Loss tangent [tan (α)].

Some noticeable variations in the 9.2- to 9.8-GHz frequency range are indicated in Fig. 2, however, from the average values of ϵ and μ. Furthermore, values (missing in Fig. 2) obtained at three frequencies were erroneous. These errors are attributed to the fact that the network analyzer signal source was not frequency stabilized at the time measurements were obtained on the Teflon material.[4] Without a frequency-stabilized signal source, the frequencies at the time of measurement do not exactly repeat those at the time of calibration, which produces errors in the phase of the measured scattering parameters. The accuracy of the values of complex ϵ and μ depends significantly on the accuracy of the measured scattering parameter phase data.

The Eccosorb SF-5.5 is an absorber type material which resonates at 5.5 GHz. The basic composition of the material is silicone rubber presumably loaded with lossy magnetic particles. When backed with a metallic surface, the material is reported to be effective in absorbing a normally incident wave at 5.5 GHz, although some absorption occurs at other frequencies and other angles of incidence as well. The requirement of a metallic surface backing suggests that the absorber is a magnetically lossy material which absorbs the high currents existing along the metallic surface excited by the incident wave. That the material is magnetically lossy is confirmed by Fig. 3 which indicates a value of μ_r'' greater than zero over X band. Fig. 3 also indicates that the material is not electrically lossy ($\epsilon_r'' \cong 0$ over the band) but does have a relatively high dielectric constant ($\epsilon_r' \cong 13.7$ over the band). Furthermore, μ_r' is greater than 1.0, varying from about 1.9 to 1.4 over the band. Attenuation and loss tangent[5] are shown in Fig. 4 for the Eccosorb material. Attenuation varies from about 24 to 40 dB/cm and loss tangent from about 0.7 to 0.9 over X band.

[4] A frequency-stabilized signal source was used, however, for the Eccosorb SF-5.5 measurements.

[5] Loss tangent ($\tan\delta = \mu_r''/\mu_r'$ since $\epsilon_r'' = 0$.

Complex ϵ and μ data have been presented for two commercially available dielectric materials as examples of results obtained using the automatic measurement system described in this paper. This system, however, has also been found useful in determining the dielectric properties of rock, soil, and other nonstandard materials.

Acknowledgment

The author wishes to thank Dr. L. Young and L. A. Robinson for many helpful suggestions and encouragements during the development of the automatic measurement system and related data processing techniques.

References

[1] L. A. Robinson, W. B. Weir, and L. Young, "Location and recognition of discontinuities in dielectric media using synthetic RF pulses," this issue, pp. 36–44.

[2] A. R. Von Hipple, Ed., *Dielectric Materials and Applications*. New York: Wiley, 1954.

[3] A. R. Von Hipple, *Dielectric and Waves*. New York: Wiley, 1954.

[4] S. Ramo and J. R. Whinnery, *Fields and Waves in Modern Radio*, 2nd. ed. New York: Wiley, 1953, ch. 8.

[5] W. E. Milne, *Numerical Calculus*. Princeton, N. J.: Princeton Univ. Press, 1949, ch. IV.

[6] S. B. Cohn, "Confusion and misconceptions in microwave engineering," *Microwave J.*, vol. 11, p. 20, Sept. 1968.

[7] A. M. Nicolson and G. F. Ross, "Measurement of the intrinsic properties of materials by time-domain techniques," *IEEE Trans. Instrum. Meas.*, vol. IM-19, pp. 377–382, Nov. 1970.

Reprinted from
Proceedings of the IEEE
Volume 62, No. 1, Jan., 1974

pp. 33-36
PRINTED IN THE U.S.A.

REFERENCES

Cooper, D. W., J. E. Heighway, D. F. Shook, R. J. Jirberg, and R. S. Vickers, "Remote Profiling of Lake Ice Thickness Using a Short Pulse Radar System Aboard a C-47 Aircraft," Proc. IEEE Symposium on Earth Environment and Resources, Philadelphia, Pa., 1974.

Vernier, G. O., and F. R. Cross, "An Experimental Look at the Use of Radar to Measure Snow and Ice Depths," CRC Technical Note No. 646, Communications Research Center, Department of Communications, Ottawa, Canada (November 1972).

Von Hippel, A. R., Dielectrics and Waves (John Wiley & Sons, Inc., New York, N. Y., 1954).

Cumming, W. A., "The Dielectric Properties of Ice and Snow at 3.2 cm," J. Appl. Phys., Vol. 23 (7 July 1952).